Chemical Science

ROYAL SOCIETY OF CHEMISTRY

EDGE ARTICLE

View Article Online
View Journal

Cite this: DOI: 10.1039/d5sc10233b

All publication charges for this article have been paid for by the Royal Society of Chemistry

Received 31st December 2025
Accepted 25th March 2026

DOI: 10.1039/d5sc10233b

rsc.li/chemical-science

Synthesis of bacteriochlorophyll *a*

Duy T. M. Chung, Khiem Chau Nguyen, † Yizhou Liu and Jonathan S. Lindsey *

Photosynthetic tetrapyrroles absorb light to power the biosphere but have largely been neglected as targets of chemical synthesis. Bacteriochlorophyll *a* – a key macrocycle in the bacterial photosynthetic reaction center – contains four stereocenters at the rim of the bacteriochlorin chromophore due to the *trans*-dialkyl group in each pyrroline ring (B, D), and an epimerizable β-ketoester embedded in the isocyclic ring (E). Here, each pair of stereodefined vicinal substituents was introduced as a chiral 4-nitroalkanal building block, which was converted to an alkynone for subsequent coupling with an iodopyrrole (A, C), affording the AD and BC dihydrodipyrrins. The dihydrodipyrrins were equipped with reactive groups (1-formyl, AD-half; 1-(1,1-dimethoxymethyl) and 8-(3-methoxy-1,3-dioxopropyl, BC-half) suited for directed macrocycle formation. Knoevenagel condensation of AD and BC halves afforded a propenone, the nexus for constructing ring E concomitantly with the macrocycle in the subsequent one-flask, double-ring closure (Nazarov cyclization, electrophilic aromatic substitution, elimination of methanol). The aromatic bacteriopheophorbide was obtained as the 2-trimethylsilylethyl propanoate, which upon acidolysis and esterification with phytol yielded bacteriopheophytin *a*; subsequent magnesiation gave bacteriochlorophyll *a*. The modularity of the synthesis, straightforward construction of asymmetric building blocks, and convergent joining of AD and BC halves suggest that the present route may provide an entrée into diverse photosynthetic macrocycles.

Introduction

Bacteriochlorophylls, the chief pigments in anoxygenic photosynthetic bacteria, are of fundamental interest for a host of reasons. First, the long-wavelength absorption of bacteriochlorophyll *a* (**BChl *a***) and its free base counterpart bacteriopheophytin *a* (**Bpheo *a***) appears in the near-infrared (770 and 750 nm, respectively),[1] a spectral region of immense interest in fields ranging from energy sciences to photomedicine.[2] Second, anoxygenic photosynthetic bacteria[3] contain only a single reaction center as opposed to the tandem (Z-scheme) reaction centers that underpin chlorophyll-based, oxygenic photosynthesis of plants and cyanobacteria.[4] The comparative simplicity of the reaction center of anoxygenic photosynthetic bacteria has led to foundational use in studies of electron-transfer processes.[5–8] Third, the mechanisms of energy transfer among **BChl *a*** molecules in antenna proteins continue to challenge theorists.[9] Finally, while anoxygenic photosynthetic bacteria likely make only a small contribution to global photosynthetic productivity (given an estimated oceanic concentration of bacteriochlorophyll *a* that is ~0.1–1% of that of chlorophyll *a*),[10] a more substantial ecological role prevails in environments ranging from microbial mats (*e.g.*, Fig. 1, panel A)[11] to tropical rain forests.[12,13]

Bacteriochlorophyll *a* as a target of chemical synthesis presents several challenges, including (1) susceptibility to oxidative dehydrogenation to give the chlorin or porphyrin; (2) the presence of four stereocenters, two in each pyrroline ring;[14] and (3) the presence of the annulated, "isocyclic" ring E. Given the absence of total synthesis, analogues have been prepared given the wide interest in photochemical processes undergirded by bacteriochlorophylls. Thus, use of native **BChl *a*** as a starting point for semisynthesis[15] has afforded selected derivatives albeit in minute amounts. Isotopic feeding experiments with photosynthetic bacteria can afford exhaustive or partial,[16,17] but not single-site (C, N, O), isotopic incorporation in the macrocycle, which could be pivotal in magnetic resonance experiments of photosynthetic complexes.[18] Alterations to the bacterial photosynthetic reaction centers to tune electron-transfer processes have focused on modification of the protein superstructure much more than the ostensibly simpler native pigments. Model bacteriochlorins have been prepared by *de novo* synthesis[19–21] but lack the full structural richness of the native macrocycles. The synthetic lacuna outlined for **BChl *a*** – a macrocycle first reported in the 1930s[22] – is not a singularity, as the entire class of photosynthetic tetrapyrroles has fallen outside the realm of interest in modern natural products synthesis.[23]

In this paper, we report the synthesis of bacteriopheophorbide *a* (**Bpheide *a***), methyl bacteriopheophorbide *a* (**Me-BPheide *a***), bacteriopheophytin *a* (**Bpheo *a***), and bacteriochlorophyll *a* (**BChl *a***) starting from simple and readily

Department of Chemistry, North Carolina State University, Raleigh, NC 27695-8204, USA. E-mail: jlindsey@ncsu.edu

† Deceased.

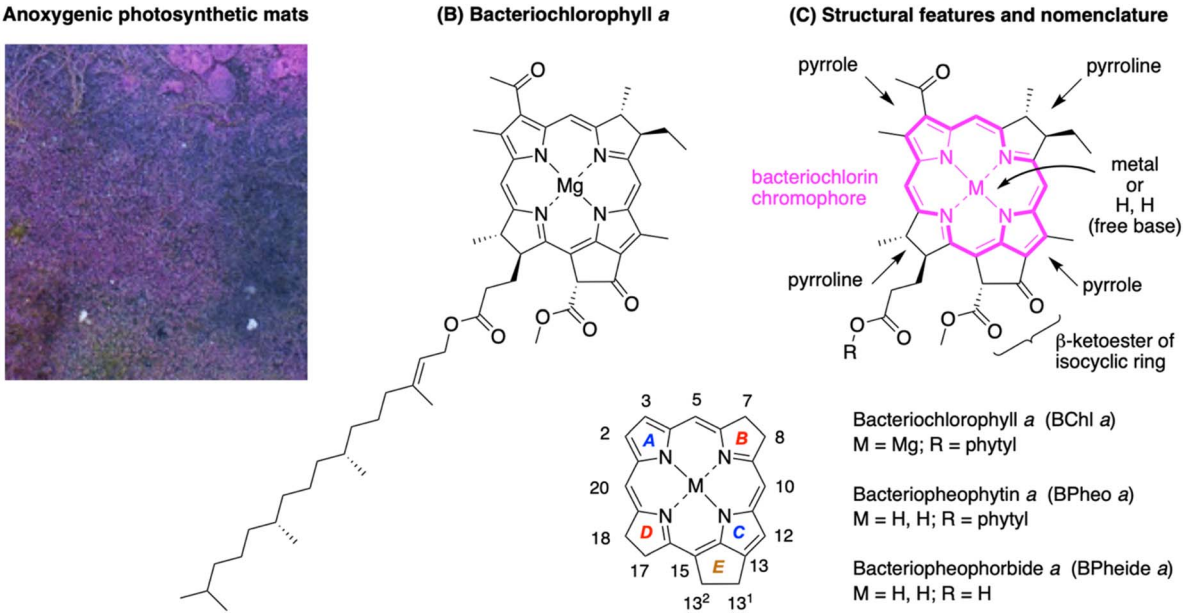

Fig. 1 (A) Microbial mats containing anoxygenic photosynthetic bacteria.[11] (B) Bacteriochlorophyll *a*. (C) Key motifs and nomenclature showing rings A–E.

available building blocks (Fig. 1, panels B and C). The terminology "bacterio" indicates the *trans*-tetrahydroporphyrin chromophore, "*a*" indicates the macrocycle family member, "pheo" indicates the free base macrocycle, and "phorbide" and "phytin" refer to the nature of the substituent (R) at the 17^3-carboxylic acid. The magnesium chelate of **Bpheide *a*** (bacteriochlorophyllide *a*) is the last biosynthetic precursor to all structural variants of **BChl *a***,[24,25] which differ by esterification with diverse hydrocarbon alcohols (ROH).[26] Such a synthetic strategy should provide a general framework for gaining access to the family of ~20 photosynthetic tetrapyrrole macrocycles.

Results and discussion

Retrosynthesis

Two key features of the synthesis entail (i) establishment of the stereochemical configuration of substituents in precursors to the pyrroline rings at an early stage of the synthesis with reliance on established asymmetric synthetic methodology, and (ii) joining of AD and BC halves *via* a two-step sequence: Knoevenagel condensation followed by a double-ring closure process consisting of Nazarov cyclization, electrophilic aromatic substitution, and elimination of methanol. The nascent isocyclic ring E, formed *via* successive Knoevenagel and Nazarov reactions, guides the appropriate joining of the AD and BC halves. The retrosynthesis is shown in Fig. 2.

The synthesis of pyrroles (rings A and C) is well established.[27,28] Routes to the pyrrolines (rings B and D) have relied on access to chiral hexynones[29–31] that upon joining with the pyrrole afford the dihydrodipyrrin (AD or BC) bearing the *trans*-dialkyl substituents. The prior route to chiral hexynones used the Schreiber-modified Nicholas reaction.[32,33] Here, an asymmetric Michael addition of an aliphatic aldehyde and nitroalkene (**1**, **3**) is reported as a means to set the contiguous stereocenters in a chiral nitroaldehyde (**2**, **4**) (Fig. 2). The new route proceeds with fewer protecting groups and enables direct

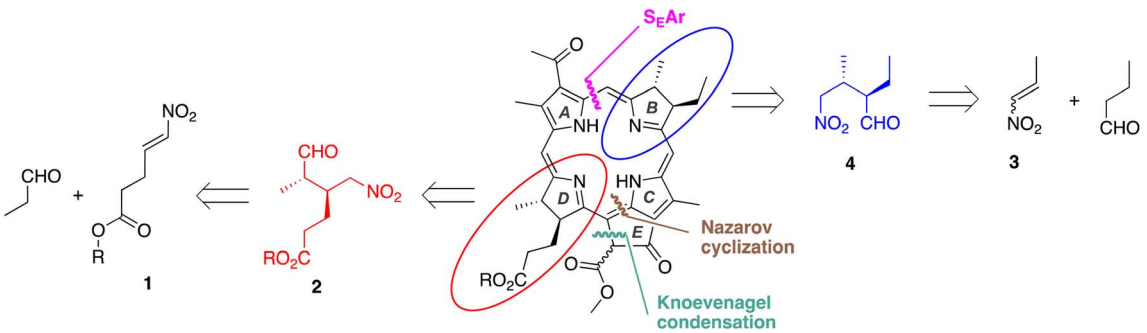

Fig. 2 Retrosynthesis. Vicinal stereocenters in rings B (blue) and D (red) are created *via* asymmetric Michael reaction of a nitroalkene (**1**, **3**) and an aldehyde (propanal or butanal). The resulting AD and BC halves are joined *via* Knoevenagel condensation, Nazarov cyclization, and electrophilic aromatic substitution (S$_E$Ar).

introduction of the propanoic acid unit on ring D (which previously required resort to a protected propanol[31]).

Chiral precursors to pyrroline rings B and D

The synthesis of nitroalkenes **1** and **3** is shown in Fig. 3 panels A and B, respectively. Succinic anhydride was treated with 2-(trimethylsilyl)ethanol in the presence of triethylamine and a catalytic amount of 4-dimethylaminopyridine (DMAP)[34] to give the mono-ester. A two-step one-flask procedure with 1,1′-carbonyldiimidazole followed by nitromethane gave the α-nitroketone.[35] Reduction with sodium borohydride[35] followed by dehydration of the resulting alcohol with methanesulfonyl chloride and triethylamine[36] at low temperature provided nitroalkene **1**, a stable compound isolated as an orange oil (see the absorption spectrum in Fig. S1). The nitroalkene **1** was synthesized *via* a streamlined manner and the above reactions were readily performed in multigram scale. The preparation of nitroalkene **3** began with the KF-catalyzed condensation of nitromethane and acetaldehyde to obtain the nitroalcohol,[37] which was subjected to esterification, elimination, and distillation in one setup (Fig. S2).[38] The distillate contained the desired **3** (along with water), which could be dried over Na_2SO_4 and stored at −20 °C under argon in the dark for several months without any significant degradation.

The conditions for the Michael reaction of each nitroalkene and aldehyde were surveyed with use of chiral HPLC of reaction aliquots, with knowledge that the α-position of aliphatic aldehydes is easily epimerized[39–41] upon prolonged reaction and purification by column chromatography.[42–44] For these specific substrates, the best conditions were found to be those of Zhu[45] – in aqueous solution containing benzoic acid at 0 °C for 2–3 hours in the presence of an *O*-TMS-protected diphenylprolinol (Hayashi)[44] catalyst (2 mol%). Thus, nitroalkene **1** and propanal in the presence of (*R*)-*O*-TMS-protected diphenylprolinol (**I**) afforded predominantly one enantiomer (**2**, Fig. 3 panel A); the elution of the four stereoisomers was established by parallel reactions with pyrrolidine (Fig. S3–S5). Similarly, nitroalkene **3** and butanal in the presence of (*S*)-*O*-TMS-protected diphenylprolinol (**II**) afforded predominantly one enantiomer (**4**, Fig. 3 panel B); the parallel reaction with pyrrolidine also showed peaks for the four expected stereoisomers (Fig. S3–S5). In both cases, use of the enantiomer of **I** or **II** enabled identification of the enantiomer of **2** or **4**, respectively, and by inference, the corresponding diastereomers (Fig. S3 and S4). Integration of the peaks gave dr = 23 : 1 and 53 : 1 for **2** and **4**, respectively. The enantiomer of **2** was not detected whereas that for **4** gave an *ee* of 99%. After aqueous quenching, nitroalkanal **2** was stable at 0 °C under argon in the dark for several months without any significant epimerization, while nitroalkanal **4** underwent epimerization under the same conditions.

Synthesis of the AD half and the BC half

The asymmetric Michael addition of nitroalkene **1** and propanal was carried out to give chiral aldehyde **2**, which was used without chromatography in subsequent reactions (Fig. 4 top panel). To confirm the stereochemistry, conversion to the

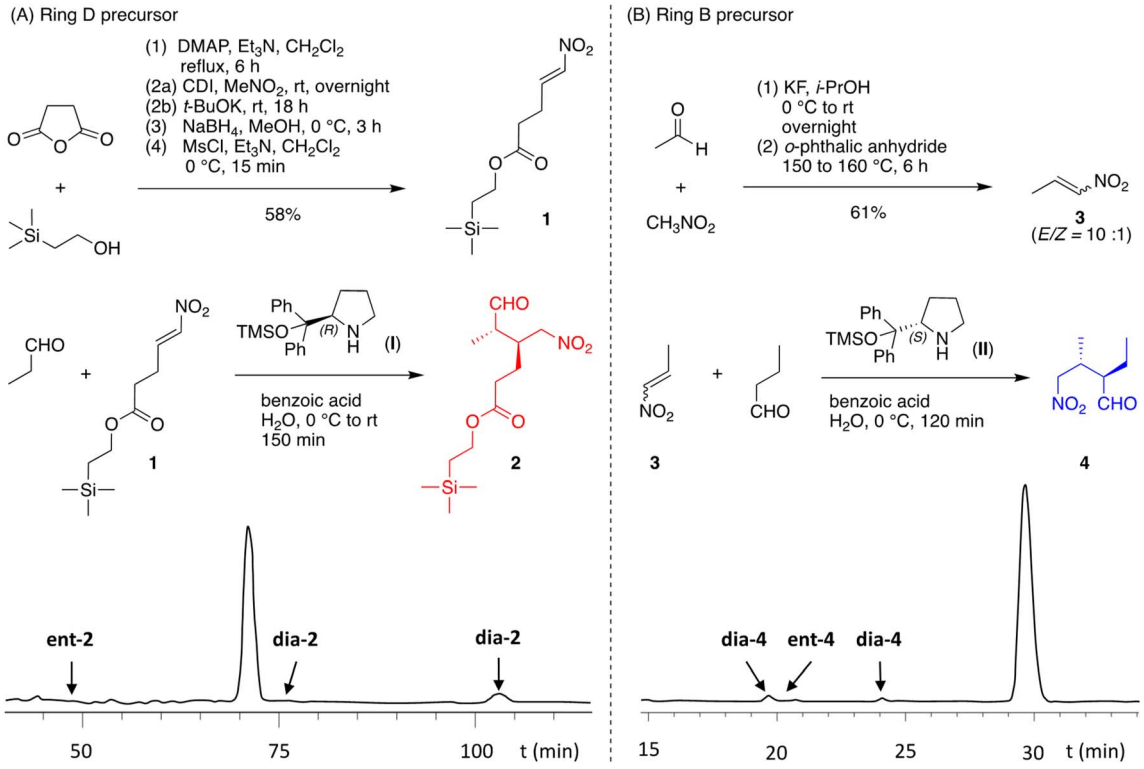

Fig. 3 Synthesis of nitroalkenes and asymmetric Michael addition to install two contiguous stereocenters; examination by chiral HPLC with far-UV detection (see the experimental section for conditions). Panel A: ring D precursor **2**. Panel B: ring B precursor **4**.

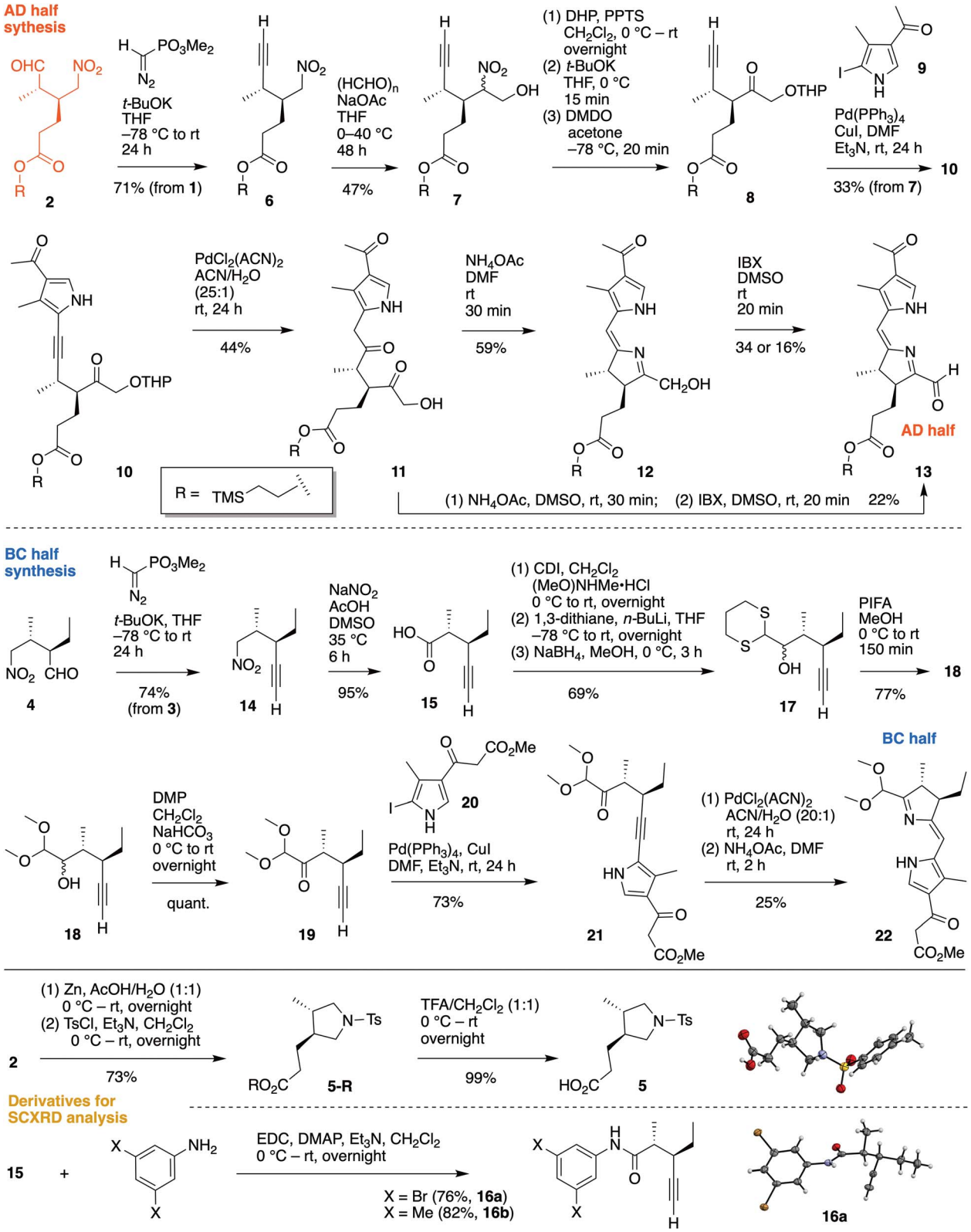

Fig. 4 Synthesis of the AD half (upper panel) and the BC half (middle panel). The preparation of derivatives and resulting single-crystal X-ray structures (lower panel) validated the desired *trans*-dialkyl stereochemistry in each case.

pyrrolidine **5-R** (by reduction of the nitro group, reductive amination, and tosylation)[46] followed by removal of the 2-(trimethylsilyl)ethyl group[47] gave **5** as a solid, which upon SCXRD analysis showed the desired *trans*-(*S*),(*S*) stereochemistry (Fig. 4 bottom panel, Fig. S6 and Table S1). The crude **2** was immediately treated with the Seyferth–Gilbert reagent (dimethyl

(diazomethyl)phosphonate)[48,49] to give alkyne **6** in 71% yield (from nitroalkene **1**). Subsequent nitro–aldol reaction in the presence of paraformaldehyde under mild basic condition[50] gave nitro-substituted chiral heptynoate **7** in 47% yield (and recovered starting material **6** in 45% yield).

Attempts to transform the nitroalkyl moiety of **7** to the ketone (Nef reaction) under diverse conditions (*e.g.*, NaOH and $KMnO_4$,[51] $NaNO_2$,[52] *tert*-BuOK and DMDO[53]) afforded complex mixtures due to fragmentation, over-oxidation, and isomerization between α-ketol and α-hydroxyaldehyde species. To sidestep possible reactions of the unprotected alcohol, **7** was treated with 3,4-dihydro-2*H*-pyran and catalytic pyridinium *p*-toluenesulfonate[54] to obtain the tetrahydropyranyl (THP) ether. Subsequent Nef reaction,[53] entailing exposure to *tert*-BuOK in anhydrous THF and oxidation with DMDO, afforded upon silica pad filtration crude **8**, which was used directly in the next step (Fig. 4 top panel). An analogue of compound **8** with R = phytyl was previously synthesized (*via* the propanol substituent)[31] in exploratory studies.

The Sonogashira coupling[30,55,56] of chiral heptynoate **8** and pre-A pyrrole **9** (ref. 57) gave heptynylpyrrole **10** in 33% yield (from **7**). Treatment of **10** with $PdCl_2(MeCN)_2$ (ref. 58) in aqueous acetonitrile for anti-Markovnikov hydration of the internal alkynyl group gave the expected 1,4-diketone along with cleavage of the THP ether (as is known to occur[59]). Despite the moderate yield of the hydration (44%), attempts to characterize components other than **11** in the reaction mixture were unfruitful. The anti-Markovnikov hydration affording **11** was confirmed by nOe correlation between protons on the pyrrolic 3-methyl group and the 2-methylene group, and the absence of COSY correlation of protons on the 2-methylene group with other protons at different positions.

The Paal–Knorr type cyclization[60] of **11** upon treatment with NH_4OAc in anhydrous DMF at room temperature gave 1-hydroxymethyl dihydrodipyrrin **12** in 59% yield (Fig. 4 top panel). Monitoring the reaction by UV-vis absorption spectroscopy (Fig. S7, panel A) afforded spectra wherein the peak at 275 nm for **11** gave way over 30 min to a more intense peak at 325 nm for **12**. Oxidation of the primary alcohol of **12** with IBX[61] in anhydrous DMSO at room temperature[62] gave the AD half **13** in 34% yield (0.22 mmol-scale) or 16% yield (2.6 mmol-scale). The conversion was similarly monitored by UV-vis absorption (Fig. S7, panel B). The absorbance at 325 nm (hydroxymethyl **12**) decreased whereas a new peak emerged at 425 nm (aldehyde **13**) after 20 min of exposure to IBX. Prolonging the reaction time for both reactions showed a decrease of the characteristic absorbance peaks (325 nm for **12**, and 425 nm for **13**; see Fig. S8 and S9).

The low yield of the conversion of dihydrodipyrrin **12** to **13** may be attributed to several factors. First, reactant and product can each independently give rise to a dipyrromethane (upon tautomerization) or a dipyrrin (upon oxidation). Secondly, 1-carboxaldehyde **13** can undergo self-condensation under the acidic conditions generated by IBX by-products (*e.g.*, 2-iodobenzoic acid, 2-iodosobenzoic acid[63]). Third, dihydrodipyrrin **12** is a vinylogous pyrrole-α-carbinol, which as a class are known to be quite reactive toward hydroxyl elimination and polymerization. The α-carbinol **12** decomposed readily under anaerobic conditions and minimal light at −20 °C with detectable degradation (^{1}H NMR and UV-vis analysis) within 24 h. In contrast, the oxidized product **13** remained stable under identical conditions for several months. In an effort to sidestep such pitfalls, a streamlined conversion of **11** to **13** was attempted; however, the combined yield of the final two reactions did not improve (not shown here). On the other hand, changing the solvent of the Paal–Knorr reaction from DMF to DMSO with all other parameters constant afforded an increase in overall yield of the two aforementioned reactions.

The synthesis of the BC half[30] began with the homologation[48,49] of the 5-nitropentanal **4** to obtain volatile nitropentyne **14** on a gram scale in 74% yield (Fig. 4 middle panel). The nitro group in **14** was converted to the carboxylic acid **15** by treatment with $NaNO_2$ (3 equiv) in DMSO and AcOH[64] (95% yield). Two anilide derivatives of **15** were isolated as solids (**16a**, **16b**), which upon SCXRD analysis confirmed the desired *trans*-(*R*),(*R*) stereochemistry (Fig. 4 bottom panel, Fig. S10a, b and Tables S2a, b). Treatment of a CH_2Cl_2 solution of **15** with CDI and (MeO)NHMe·HCl afforded the Weinreb amide, which underwent a 2-step one-flask procedure (Corey–Seebach reaction, reduction with $NaBH_4$) to give dithianylalcohol **17** (69% over 3 steps). Oxidative transacetalization[65] of the dithiane moiety with (bis(trifluoroacetoxy)iodo)benzene (PIFA) afforded the dimethoxy group in **18** in good yield. Finally, treatment of **18** with DMP gave the chiral hexynone **19**, which serves as the pre-B unit. In a similar manner as for the BC half, alkynone **19** underwent Sonogashira coupling with iodopyrrole pre-C (**20**)[27] to obtain the hexynylpyrrole **21** in good yield. The anti-Markovnikov hydration of **21** following by Paal–Knorr type cyclization gave BC-half **22** in 25% yield. The present route provides superior access to the known BC half[30] in terms of chiral precursor **4**, proof of stereochemistry (**16a**, **16b**), and streamlined procedures.

In summary, the asymmetric Michael reaction has enabled the conversion of simple starting materials to the AD and BC halves. Each compound in both routes (Fig. 4), except for crystalline derivatives **5**, **16a** and **16b** for SCXRD analyses, was obtained as an oil or paste. The small quantities of diastereomers observed in the Michael reactions were carried forward and ensuing diastereomers could be clearly discerned by ^{1}H NMR analysis for **6**, **14**, **15**, and **19** (dr = 4.9 : 1, 23 : 1, 33 : 1, and 17 : 1, respectively) (Fig. S11).

Macrocycle formation, elaboration, and characterization

Model studies of the Knoevenagel condensation and subsequent double-ring closure have been carried out wherein one or both AD/BC halves contains gem-dimethyl substituents,[21,28,29,66,67] which have identified promising conditions, albeit not with the full complement of stereodefined substituents. The Knoevenagel condensation (40 mM each half) relies on mild relatively neutral-basic conditions at room temperature, whereas the double-ring closure relies on mild acidic conditions at 80 °C.

Here, the AD half (**13**) and the BC half (**22**), which collectively contain six carbonyl groups or equivalents, were treated to Knoevenagel condensation[68] (Fig. 5 panel A). Application of the standard conditions (piperidine, AcOH, 3 Å MS, acetonitrile, room temperature for 20–60 h), which gave up to 73% with substrates containing simple substituents in the AD and BC halves,[28] gave 11% here upon reaction of **13** and **22**. Microscale screening of the conditions drawn from the literature[66,69–73] of the Knoevenagel reaction with **13** and **22** in 1 : 1 ratio (~2 μmol each) at room temperature (see Table S3) gave the following observations: (1) under basic conditions (only piperidine), no product was detected, while using piperidine in conjunction with acetic acid gave low yield after prolonged reaction time. (2) Use of catalysts derived from amino acids gave low yield or no product. (3) A synergistic effect of pyrrolidinium acetate and $Mg(OTf)_2$ was found to give a moderate yield of enone **23** as well as unreacted BC half **22**. The latter conditions were thus employed in the synthesis. Reaction at 0.3 mmol each at room temperature for 24 h gave Knoevenagel enone **23** as an orange solid (see absorption spectrum in Fig. S12) in 35% yield. Examination by ^{1}H NMR spectroscopy suggested the presence of only one enone isomer. A deeper assessment of the *E*/*Z* ratio was not attempted because (1) prior studies of similar enones have shown an *E* : *Z* ratio >10 : 1,[29] (2) the two isomers interconvert during the subsequent Nazarov electrocyclization,[74] and (3) use of either isomer alone gives the same yield in the Nazarov cyclization.[67]

Enone **23** was treated to the acidic conditions for the double-ring closure[67] (~0.2 mM in acetonitrile containing $Yb(OTf)_3$ at 80 °C for 1 h), which gave 2-(trimethylsilyl)ethyl bacteriopheophorbide **24** in 36% yield along with a minor amount of the 2-(trimethylsilyl)ethyl (TMSE)-cleaved product, bacteriopheophorbide *a* (**Bpheide *a***, R = H). The examination of reaction samples by absorption spectroscopy (Fig. 5 panel B) showed the steady emergence of the characteristic B, Q_x and Q_y peaks[4] of the bacteriopheophorbide. Examination by reversed-phase (RP) HPLC showed the disappearance of enone **23** within 15 min and the appearance of two peaks corresponding to bacteriopheophorbide **24** (Fig. 5 panel C). The two peaks are attributed to the two configurations of the 13^2-carbomethoxy group, with *R* : *S* ratio of ~9 : 1. The configuration of the 13^2-carbomethoxy group is set upon double-ring closure.[29,67] Epimerization at the 13^2-site in this class of macrocycles is known to occur slowly on standing,[75,76] and both 13^2-epimers of the

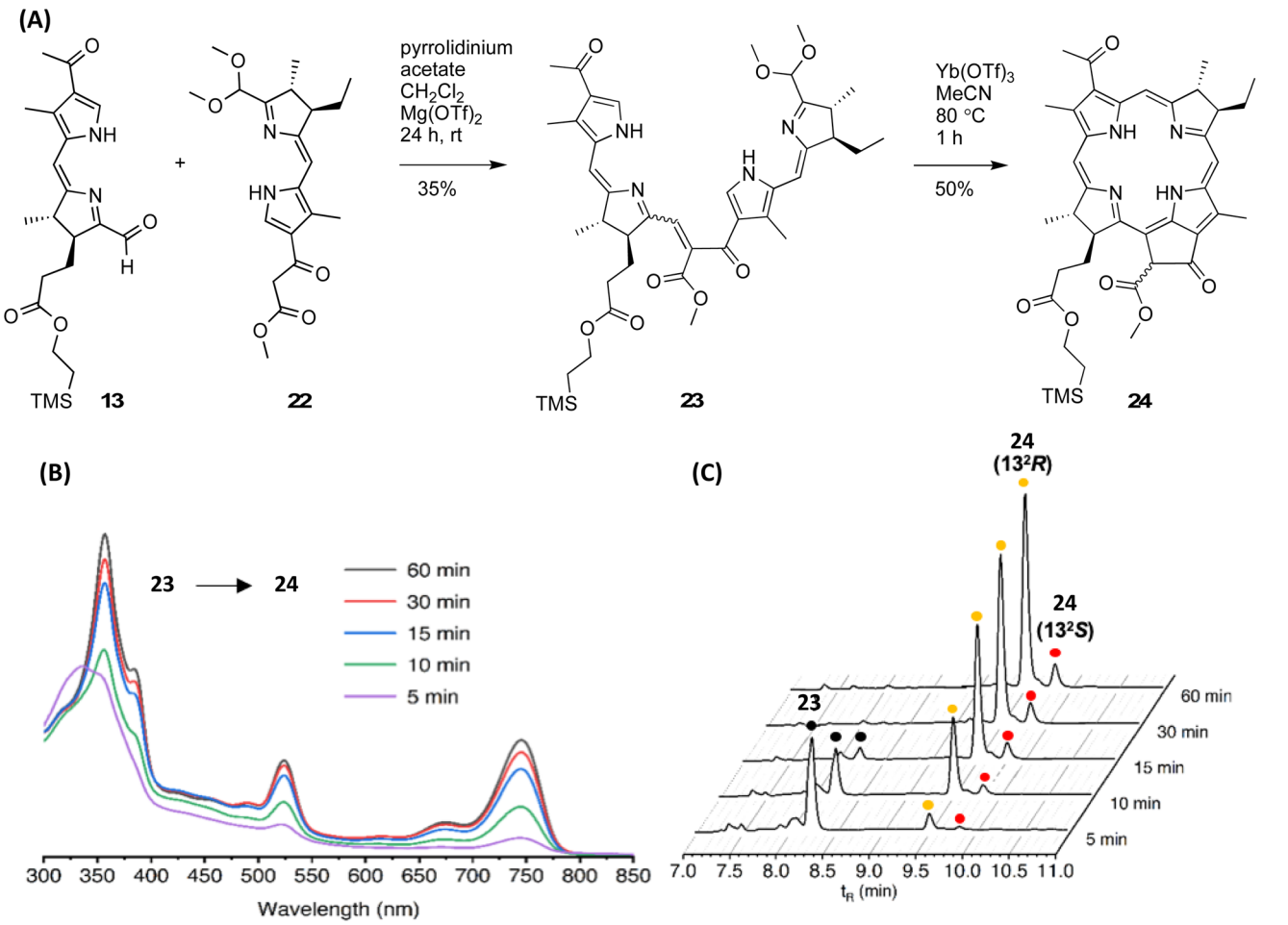

Fig. 5 Macrocycle synthesis route (A). Time course for conversion of **23** to **24** (lower panels): (B) absorption spectra in acetonitrile at room temperature. (C) Reversed-phase HPLC data with λ_{det} = 340 nm (see experimental section for conditions).

macrocycles are employed in native photosynthetic systems,[77] although no enzyme for epimerization is known.[78] The two epimers could be partially separated by preparative TLC and assessed by RP-HPLC (Fig. S13). Workup and isolation of bacteriopheophorbide **24** (combined epimers) from the reaction mixture entailed dilution with dichloromethane, washing with neutral aqueous phosphate buffer solution, concentration of the organic phase, and reversed-phase column chromatography under argon and dim lighting. Attempts to use normal phase (silica) chromatography resulted in the well-known processes of allomerization and adventitious dehydrogenation yielding multiple products (Fig. S14).

Removal of the 2-(trimethylsilyl)ethyl protecting group of bacteriopheophorbide **24** with TBAF or other conditions proved difficult (Fig. S15 and S16), but could be accomplished with neat trifluoroacetic acid (TFA) to give **Bpheide *a*** in 83% yield (Fig. 6 panel A). Subsequent transformations rely heavily on established procedures developed over the years for semisynthesis and reconstitution of native-origin macrocycles. Bacteriopheophorbide **24** also was treated with TFA followed by esterification (as described by Wasielewski and Svec[79]) of the resulting 17^3-carboxylic acid with an alcohol in the presence of benzotriazole-1-methanesulfonate (BtOMs)[80] and triethylamine; use of methanol gave methyl bacteriopheophorbide *a* (**Me-Bpheide *a***) whereas native phytol (for which syntheses are known[81]) gave bacteriopheophytin *a* (**Bpheo *a***).

The free base macrocycle **Bpheo *a*** was treated to established conditions for magnesiation,[82] which entail lithium 2,2,6,6-tetramethylpiperidide (LiTMP) and iodomagnesium 2,6-di-*tert*-butyl-4-methylphenolate (I-Mg-BHT) in thiophene, to afford

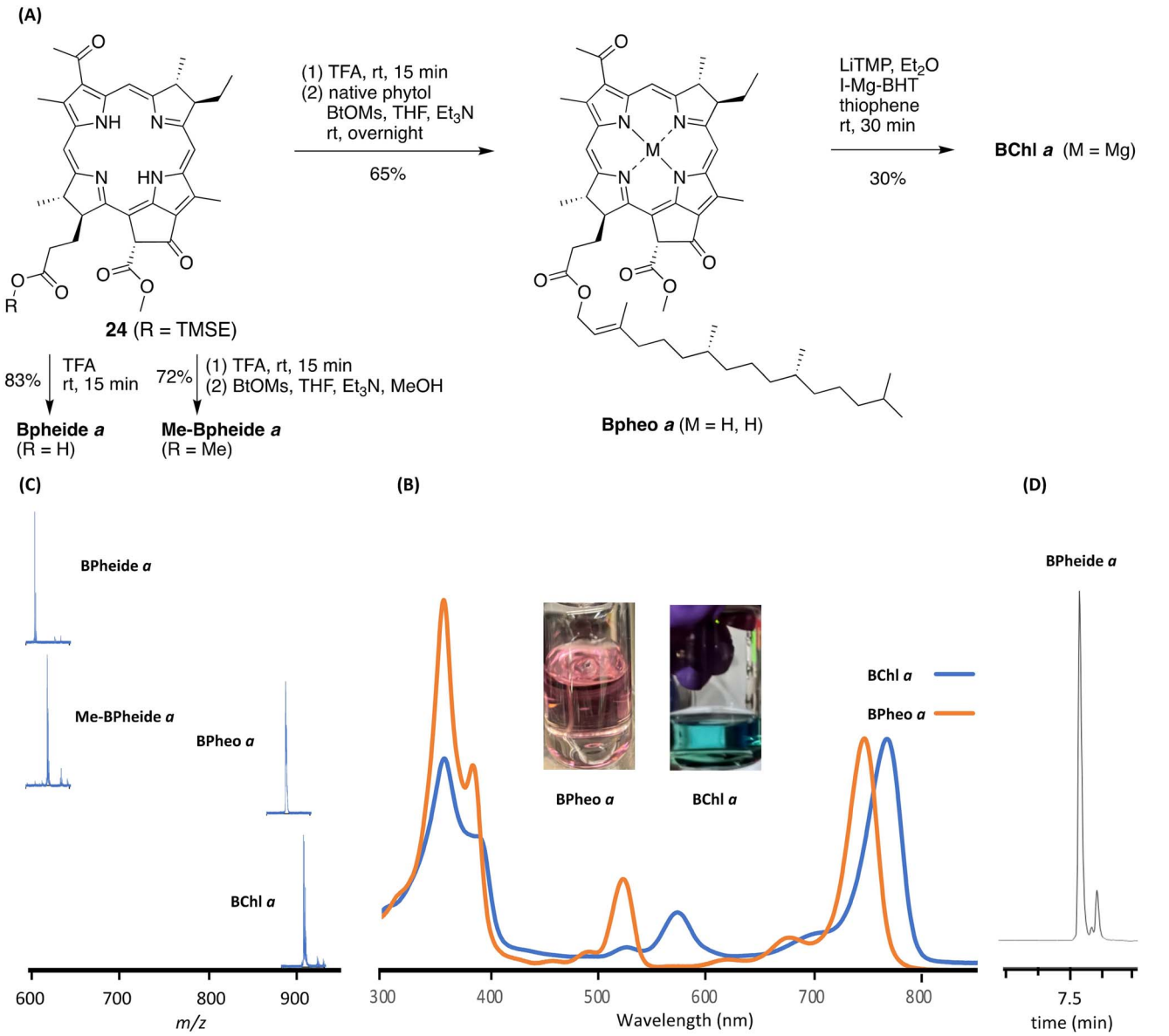

Fig. 6 (A) Macrocycle elaboration. (B) Absorption spectra in diethyl ether at room temperature of **Bpheo *a*** and **BChl *a*** (normalized at the Q_y bands). Insets are photos of dilute solutions. (C) MALDI-MS data of molecular ion region (see experimental section for matrices). (D) RP-HPLC chromatogram (λ_{det} = 740 nm) of **Bpheide *a*** (see experimental section for conditions).

bacteriochlorophyll *a* (**BChl *a***). The long-wavelength absorption of the reaction mixture red-shifted over 30 min as expected for magnesiation. Prolonging the reaction did not give full conversion of the starting material, as also reported by Wasielewski.[82] Purification by reversed-phase chromatography gave **BChl *a***, which displayed absorption bands (Fig. 6 panel B) in the spectral regions of the near-ultraviolet (359, 390 nm, B band), green (575 nm, Q_x band), and near-infrared (770 nm, Q_y band). The absorption spectrum was essentially identical with an authentic (commercial) sample of **BChl *a*** (Fig. S17) – including the ratio of the intensity of the Q_y band and the maximum of the B bands (I_{Q_y}/I_B),[83] a longstanding metric – and was clearly distinct from the free base precursor **Bpheo *a***. Indeed, dilute solutions of **Bpheo *a*** and **BChl *a*** appeared reddish purple and bluish-green, respectively (Fig. 6 panel B).

The free base macrocycles (**24**, **BPheide *a***, **Me-BPheide *a***, **Bpheo *a***) were characterized by a variety of methods including absorption spectroscopy, ^{1}H NMR and ^{13}C{^{1}H} NMR spectroscopy, MALDI-MS, and HRMS. The absorption spectra for all the macrocycles are provided in Fig. S18 with key parameters listed in Table S4 including comparison with native-origin samples.[84–86] Tetrapyrrole macrocycles upon MALDI-MS analysis can ionize by electron loss to form $[M^{\bullet}]^+$ as well as by protonation to form $[M+H]^+$.[87,88] The molecular ion regions are shown for **Bpheide *a*** ($C_{35}H_{38}N_4O_6$), **Me-BPheide *a*** ($C_{36}H_{40}N_4O_6$), **Bpheo *a*** ($C_{55}H_{76}N_4O_6$), and **BChl *a*** ($C_{55}H_{74}N_4O_6Mg$) by MALDI-MS with peak maxima consistent with the target macrocycles at m/z = 610.21, 624.64, 887.25, and 910.65, respectively (Fig. 6 panel C). The MALDI-MS data for **Bpheo *a*** and **BChl *a*** were essentially identical with samples of native origin. Full mass spectra are provided in Fig. S19.

RP-HPLC analysis with detection at 740 nm of **Bpheide *a*** showed a major band and a minor band (85 : 15 ratio) (Fig. 6 panel D), which are assigned to the well-known epimers that arise from the configuration of the 13^2-carbomethoxy group, as described earlier for **24**. Analysis at 440 nm, where the absorption of bacteriopheophorbins is weak (ε ~3000 M^{-1} cm^{-1}, ~1/30th of the value at 740 nm),[89,90] still showed dominant peaks

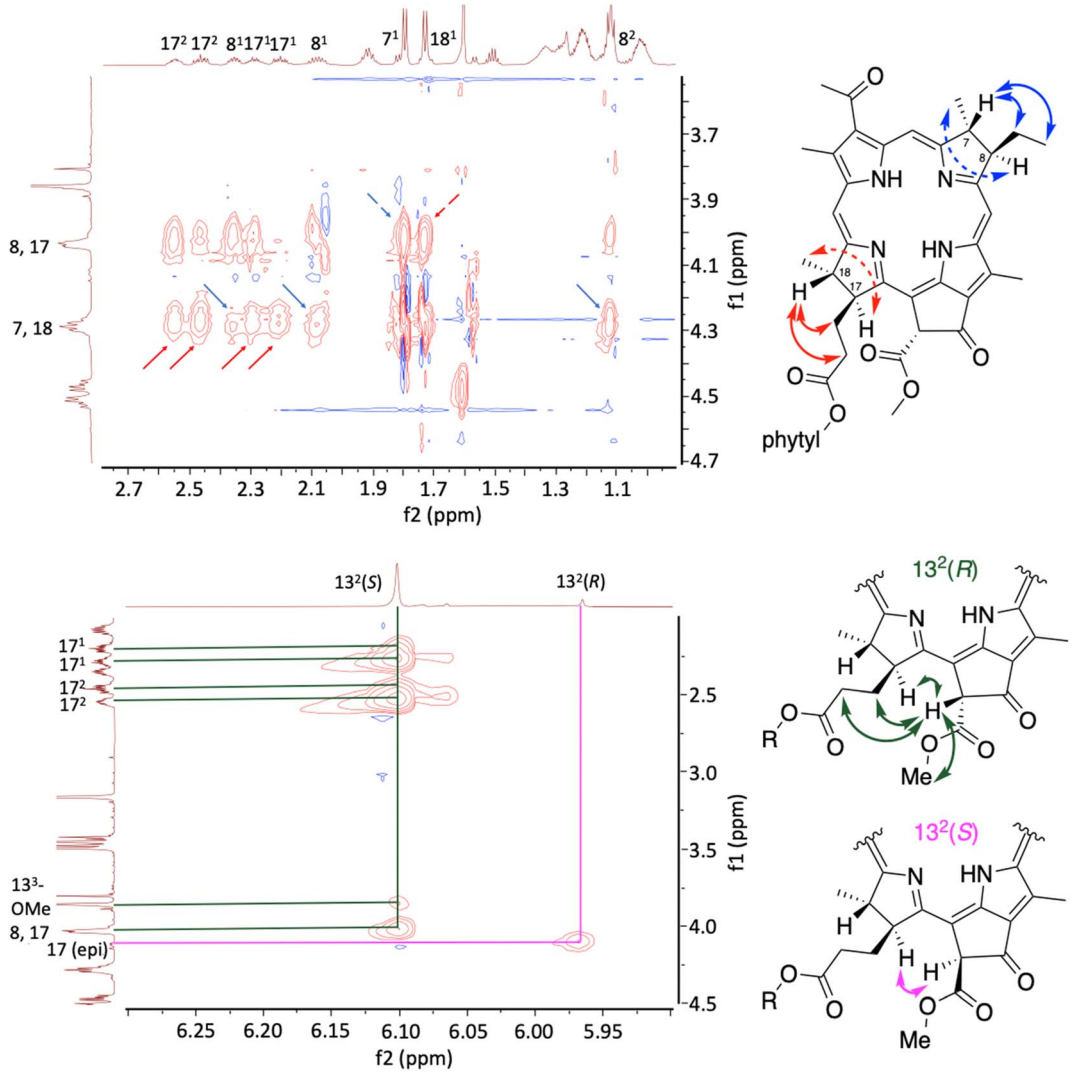

Fig. 7 Characterization of **Bpheo *a*** ($CDCl_3$ at room temperature) by ^{1}H NMR spectroscopy including ROESY analysis. (A) Selected interactions pertinent to the configuration of vicinal dialkyl groups in rings B and D. (B) Identification of (expected) epimers at the 13^2-position (R = phytyl).

due to **Bpheide *a*** albeit preceded by several trace peaks (see Fig. S20 for full RP-HPLC traces at 740 nm and 440 nm). Similar RP-HPLC analysis of **Bpheo *a*** and a native-derived sample of **Bpheo *a*** exhibited nearly identical traces although the resolution was limited given the hydrophobicity of the phytyl tail (Fig. S21).

Attempts to use CD spectroscopy of both native-derived and synthetic samples of **Bpheo *a*** were largely uninformative (Fig. S22), given the predicted cancellation of the contributions to optical activity of the stereocenters in rings B and D, leaving only the asymmetry at the 13^2-position as contributive.[91] While CD spectroscopy is attractive, more in-depth molecular information can be obtained by NMR spectroscopy.

The NMR spectral features of several members of the family of native bacteriochlorophylls including **BPheo *a*** (ref. 92–95) and **BChl *a*** (ref. 96 and 97) have been described. ^{1}H NMR spectra (in $CDCl_3$) were collected for **24**, **Bpheide *a***, **Me-Bpheide *a***, and **Bpheo *a***. The spectra were generally consistent with expectations and literature values (where comparisons could be made). The ^{1}H NMR and $^{13}C\{^1H\}$ NMR spectra of synthetic and native-derived **Bpheo *a*** samples were nearly identical (Fig. S23). The ROESY analysis for **Bpheo *a*** are shown in Fig. 7 (see Fig. S24a and b for ROESY of **24** and **Bpheide *a***). The key observations are as follows:

(1) Dialkyl configurations in rings B and D: the methine proton at the 7-position (δ = 4.27–4.31 ppm) interacted (denoted as full arrow) with the methylene protons at the 8^1-position (δ = 2.05–2.57 ppm) and the methyl protons at the 8^2-position (δ = 1.10–1.29 ppm). Similarly, the proton at the 8-position (δ = 4.02–4.05 ppm) showed an NOE-correlation (denoted as dashed arrow) with the methyl protons at the 7^1-position (δ = 1.79 ppm). Corresponding interactions were observed for the methine proton at the 18-position (δ = 4.27–4.31 ppm) with the methylene protons at the 17^1, 17^2-positions (δ = 2.05–2.57 ppm); the 17-position proton (δ = 4.02–4.05 ppm) also showed a NOE-correlation with the methyl protons at the 18^1-position (δ = 1.72 ppm). In short, the spectral data are consistent with the *trans*-relationship of the vicinal alkyl substituents within pyrroline rings B and D.

(2) Epimers at the 13^2-position. Two distinct singlets (δ = 6.10 ppm, major; 5.96 ppm, minor, with major/minor ratio of 1 : 0.16) were assigned to the 13^2-methine proton. The major signal showed strong NOE-correlations with the 17^1, 17^2-protons of the propanoate group, consistent with a *trans*-relationship of the 13^2-carbomethoxy group with the 17-propanoate tail; NOE correlations also were observed with the 17-methine proton and the 13^3-methoxy group. The minor signal did not show NOE correlations with the 17^1, 17^2-protons, suggesting a *syn*-relationship of the 13^2-carbomethoxy group with the 17-propanoate group. In short, the epimer ratio in the ^{1}H NMR spectrum mirrored that observed by RP-HPLC.

(3) Other stereoisomers. The congestion of the ^{1}H NMR spectra of the macrocycles posed challenges to the identification of diastereomers arising from any *cis*-dialkyl configurations of rings B and D. Very weak resonances can be seen in the region between the peaks assigned to the $13^2(R)$ and $13^2(S)$ protons, which are provisionally attributed to tiny quantities of diastereomers due to *cis*-dialkyl configurations in rings B and D. The H^5 resonance appears more cleanly diagnostic, as native-derived **Bpheo *a*** shows no such peaks (Fig. S25). Small quantities of *cis*-dialkyl stereoisomers are expected on the basis of the dr values (~20 : 1 and ~5 : 1; Fig. S11) of the early-stage precursors, whereas enantiomers of the respective pyrroline rings are hardly expected given the high *ee* values. In summary, the NMR data collectively support the structure and stereochemical assignment of synthetic **Bpheo *a*.**

Outlook

The work described herein achieves the total, fully traversed, synthesis of a photosynthetic macrocycle. Key features of the synthesis include the following: (1) use of established asymmetric methods to set the configurations of four stereocenters at a very early stage of the synthesis; (2) formation of dihydrodipyrrins by reaction of chiral alkynones (pre-B **19** and pre-D **8**) with 2-iodopyrroles (pre-A **9** and pre-C **20**) *via* Sonogashira cross-coupling reactions, Pd-mediated anti-Markovnikov hydration, and Paal–Knorr reaction; (3) exploitation of nascent ring E as a nexus for assembling the AD and BC halves *via* Knoevenagel reaction (mild neutral-basic conditions at high concentration) and subsequent double-ring closure (mild acidic conditions at low concentration); and (4) pre-building as much functionality into precursors thereby minimizing late-stage transformations on the intact macrocycle. The double-ring closure provides direct access to bacteriopheophorbide *a* as the 17-propanoate ester. The planning stages anticipated a host of well-precedented concerns: epimerization adjacent to carbonyl and imine groups,[39–41] tautomerization of a dihydrodipyrrin to form the dipyrromethane,[29] and oxidation[98] and/or allomerization[99] of bacteriochlorophyll macrocycles. A key conclusion is that intermediates and products could be handled securely, with the initial nitroalkanals **2** and **4** among all precursors proving to be most susceptible to epimerization, and the homologation products **6** and **14** as the most likely candidates for purification to enhance the dr values. To create desired patterns of substituents, streamlined transformations and use of a balance between early installation *versus* late-stage derivatization may be required to improve present yields such as the Knoevenagel condensation of the AD and BC halves. A key question moving forward is whether the synthetic route to bacteriochlorophyll *a* can be adapted to support synthetic entrée to the repertoire of native photosynthetic pigments as well as diverse pigment analogues. The latter include features not available from biosynthesis[24,25] or semisynthesis[15] such as single-site isotopic substitution, altered chirality, and general carbon remodeling of the macrocycle perimeter. Much synthetic work will be required to explore these possibilities.

Author contributions

D. T. M. C. and K. C. N. carried out conceptualization, investigation, and methodology. Y. L. performed the initial conceptualization. J. S. L. contributed to conceptualization, funding

acquisition, and supervision. D. T. M. C. and J. S. L. wrote the paper.

Conflicts of interest

The authors declare no competing financial interest.

Data availability

CCDC 2519170–2519172 (**16b**, **16a** and **5**) contain the supplementary crystallographic data for this paper.[100a–c]

Supplementary information (SI): full experimental section; studies of selected reactions (asymmetric Michael addition, Knoevenagel condensation, Paal–Knorr condensation; cleavage of the TMSE group); ^{1}H NMR and ^{13}C{^{1}H} NMR spectra for all new compounds; ^{1}H NMR spectra for known pyrroles **9** and **20**; macrocycle characterization data; absorption spectra; CD spectra; HPLC chromatograms; and single-crystal X-ray diffraction data. See DOI: https://doi.org/10.1039/d5sc10233b.

Acknowledgements

This work was supported by a grant from the NSF (CHE-2348052). NMR and mass spectrometry measurements were carried out in the Molecular Education, Technology, and Research Innovation Center (METRIC) at NC State University as well as at UNC Mass Spectrometry Core Laboratory. SCXRD analyses were performed by Dr Phattananawee Nalaoh at University of Tennessee at Knoxville.

References

1 D. Mauzerall, in *The Photosynthetic Bacteria*, ed. R. K. Clayton and W. R. Sistrom, Plenum Press, New York, USA, 1978, pp. 223–231.
2 B. Pucelik, A. Sułek and J. M. Dąbrowski, *Coord. Chem. Rev.*, 2020, **416**, 213340.
3 H. Gest and R. E. Blankenship, *Photosynth. Res.*, 2004, **80**, 59–70.
4 H. Scheer, in *Chlorophylls and Bacteriochlorophylls*, ed. B. Grimm, R. J. Porra, W. Rüdiger and H. Scheer, Springer Netherlands, Dordrecht, 2006, vol. 25, pp. 1–26.
5 J. J. Warren, J. R. Winkler and H. B. Gray, *Coord. Chem. Rev.*, 2013, **257**, 165–170.
6 S. G. Boxer, *J. Phys. Chem. B*, 2009, **113**, 2972–2983.
7 W. Zinth and J. Wachtveitl, *ChemPhysChem*, 2005, **6**, 871–880.
8 N. C. M. Magdaong, K. M. Faries, J. C. Buhrmaster, G. A. Tira, R. M. Wyllie, C. E. Kohout, D. K. Hanson, P. D. Laible, D. Holten and C. Kirmaier, *J. Phys. Chem. B*, 2022, **126**, 8940–8956.
9 S. Badu, R. Melnik and S. Singh, *Appl. Sci.*, 2020, **10**, 6821.
10 R. Goericke, *Limnol. Oceanogr.*, 2002, **47**, 290–295.
11 C. Hubas, B. Jesus, M. Ruivo, T. Meziane, N. Thiney, D. Davoult, N. Spilmont, D. M. Paterson and C. Jeanthon, *PLoS One*, 2013, **8**, e82329.
12 A. Lehours, A. L. Jeune, J. Aguer, R. Céréghino, B. Corbara, B. Kéraval, C. Leroy, F. Perrière, C. Jeanthon and J. Carrias, *Environ. Microbiol. Rep.*, 2016, **8**, 689–698.
13 J.-F. Carrias, C. Leroy, J.-P. Aguer, X.-T. Nguyen, J. Leflaive, B. Corbara, R. Céréghino and V. E. J. Jassey, *Hydrobiologia*, 2025, **852**, 1613–1624.
14 M. Senge, A. Ryan, K. Letchford, S. MacGowan and T. Mielke, *Symmetry*, 2014, **6**, 781–843.
15 M. A. Grin and A. F. Mironov, *Russ. Chem. Bull.*, 2016, **65**, 333–349.
16 K. Czarnecki, J. R. Diers, V. Chynwat, J. P. Erickson, H. A. Frank and D. F. Bocian, *J. Am. Chem. Soc.*, 1997, **119**, 415–426.
17 S. Prakash, A. Alia, P. Gast, H. J. M. De Groot, G. Jeschke and J. Matysik, *Biochemistry*, 2007, **46**, 8953–8960.
18 P. Bielytskyi, D. Gräsing, S. Zahn, A. Alia and J. Matysik, *Appl. Magn. Reson.*, 2019, **50**, 695–708.
19 C. Brückner, L. Samankumara and J. Ogikubo, in *Handbook of Porphyrin Science*, ed. K. M. Kadish, K. M. Smith and R. Guilard, World Scientific Publishing Company, Singapore, 2012, vol. 17, pp. 1–112.
20 S. V. Dudkin, E. A. Makarova and E. A. Lukyanets, *Russ. Chem. Rev.*, 2016, **85**, 700–730.
21 V.-P. Tran, P. Wang, N. Matsumoto, S. Liu, H. Jing, P. Nalaoh, K. Chau Nguyen, M. Taniguchi and J. S. Lindsey, *J. Porphyrins Phthalocyanines*, 2023, **27**, 1502–1551.
22 C. B. van Neil and W. Arnold, *Enzymologia*, 1938, **5**, 244–250.
23 Y. Liu, S. Zhang and J. S. Lindsey, *Nat. Prod. Rep.*, 2018, **35**, 879–901.
24 D. A. Bryant, C. N. Hunter and M. J. Warren, *J. Biol. Chem.*, 2020, **295**, 6888–6925.
25 M. S. Proctor, G. A. Sutherland, D. P. Canniffe and A. Hitchcock, *R. Soc. Open Sci.*, 2022, **9**, 211903.
26 T. Mizoguchi, M. Isaji, J. Harada, Y. Tsukatani and H. Tamiaki, *J. Photochem. Photobiol. B Biol.*, 2015, **142**, 244–249.
27 P. Z. Wang, K. C. Nguyen and J. S. Lindsey, *J. Org. Chem.*, 2019, **84**, 11286–11293.
28 D. T. M. Chung, P. V. Tran, K. Chau Nguyen, P. Wang and J. S. Lindsey, *New J. Chem.*, 2021, **45**, 13302–13316.
29 K. C. Nguyen, P. Wang, R. D. Sommer and J. S. Lindsey, *J. Org. Chem.*, 2020, **85**, 6605–6619.
30 K. C. Nguyen and J. S. Lindsey, *J. Org. Chem.*, 2023, **88**, 11205–11216.
31 K. Chau Nguyen, D. T. M. Chung, P. Nalaoh and J. S. Lindsey, *New J. Chem.*, 2024, **48**, 2097–2117.
32 S. L. Schreiber, T. Sammakia and W. E. Crowe, *J. Am. Chem. Soc.*, 1986, **108**, 3128–3130.
33 K. M. Nicholas, *Acc. Chem. Res.*, 1987, **20**, 207–214.
34 M. T. Burger and P. A. Bartlett, *J. Am. Chem. Soc.*, 1997, **119**, 12697–12698.
35 S. T. Lima, T. R. Fallon, J. L. Cordoza, J. R. Chekan, E. Delbaje, A. R. Hopiavuori, D. O. Alvarenga, S. M. Wood, H. Luhavaya, J. T. Baumgartner, F. A. Dörr, A. Etchegaray, E. Pinto, S. M. K. McKinnie, M. F. Fiore and B. S. Moore, *J. Am. Chem. Soc.*, 2022, **144**, 9372–9379.

36 J. Melton and J. E. McMurry, *J. Org. Chem.*, 1975, **40**, 2138–2139.
37 R. H. Wollenberg and S. J. Miller, *Tetrahedron Lett.*, 1978, **19**, 3219–3222.
38 M. Miyashita, T. Yanami and A. Yoshikoshi, *Org. Synth.*, 1981, **60**, 101.
39 S. Forsén and M. Nilsson, in *The Carbonyl Group*, ed. J. Zabicky, John Wiley & Sons, Ltd, Chichester, UK, 1970, vol. 2, pp. 157–240.
40 J. Toullec, *Adv. Phys. Org. Chem.*, 1982, **18**, 1–77.
41 J. Wirz, *Adv. Phys. Org. Chem.*, 2010, **44**, 325–356.
42 J. Burés, A. Armstrong and D. G. Blackmond, *J. Am. Chem. Soc.*, 2011, **133**, 8822–8825.
43 K. Patora-Komisarska, M. Benohoud, H. Ishikawa, D. Seebach and Y. Hayashi, *Helv. Chim. Acta*, 2011, **94**, 719–745.
44 Y. Hayashi, *Org. Synth.*, 2017, **94**, 252–258.
45 S. Zhu, S. Yu and D. Ma, *Angew. Chem., Int. Ed.*, 2008, **47**, 545–548.
46 B. Zheng, H. Wang, Y. Han, C. Liu and Y. Peng, *Chem. Commun.*, 2013, **49**, 4561–4563.
47 L. L. Cheung, S. Marumoto, D. C. Anderson and D. S. Rychnovsky, *Org. Lett.*, 2008, **14**, 3101–3104.
48 D. Seyferth, P. Hilbert and R. S. Marmor, *J. Am. Chem. Soc.*, 1967, **89**, 4811–4812.
49 J. C. Gilbert and U. Weerasooriya, *J. Org. Chem.*, 1982, **47**, 1837–1845.
50 F. Zhang, M. Wei, J. Dong, Y. Zhou, D. Lu, Y. Gong and X. Yang, *Adv. Synth. Catal.*, 2010, **352**, 2875–2880.
51 K. Steliou and M. A. Poupart, *J. Org. Chem.*, 1985, **50**, 4971–4973.
52 A. Gissot, S. N'Gouela, C. Matt, A. Wagner and C. Mioskowski, *J. Org. Chem.*, 2004, **69**, 8997–9001.
53 W. Adam, M. Makosza, C. R. Saha-Möller and C.-G. Zhao, *Synlett*, 1998, **1998**, 1335–1336.
54 M. Miyashita, A. Yoshikoshi and P. A. Grieco, *J. Org. Chem.*, 1977, **42**, 3772–3774.
55 P. A. Jacobi, J. Guo, S. Rajeswari and W. Zheng, *J. Org. Chem.*, 1997, **62**, 2907–2916.
56 R. Chinchilla and C. Nájera, *Chem. Rev.*, 2007, **107**, 874–922.
57 P. Wang and J. S. Lindsey, *J. Org. Chem.*, 2021, **86**, 11794–11811.
58 K. Imi, K. Imai and K. Utimoto, *Tetrahedron Lett.*, 1987, **28**, 3127–3130.
59 Y.-G. Wang, X.-X. Wu and Z.-Y. Jiang, *Tetrahedron Lett.*, 2004, **45**, 2973–2976.
60 W. G. O'Neal, W. P. Roberts, I. Ghosh and P. A. Jacobi, *J. Org. Chem.*, 2005, **70**, 7243–7251.
61 M. Frigerio, M. Santagostino and S. Sputore, *J. Org. Chem.*, 1999, **64**, 4537–4538.
62 M. Frigerio and M. Santagostino, *Tetrahedron Lett.*, 1994, **35**, 8019–8022.
63 M. A. Lapitskaya, L. L. Vasiljeva and K. K. Pivnitsky, *Mendeleev Commun.*, 2008, **18**, 309–311.
64 C. Matt, A. Wagner and C. Mioskowski, *J. Org. Chem.*, 1997, **62**, 234–235.
65 G. Stork and K. Zhao, *Tetrahedron Lett.*, 1989, **30**, 287–290.
66 S. Zhang and J. S. Lindsey, *J. Org. Chem.*, 2017, **82**, 2489–2504.
67 K. C. Nguyen, P. Wang and J. S. Lindsey, *New J. Chem.*, 2021, **45**, 569–581.
68 G. Jones, *Org. React.*, 2011, **15**, 204–599.
69 M. Yamaguchi, N. Yokota and T. Minami, *J. Chem. Soc., Chem. Commun.*, 1991, 1088–1089.
70 A. Erkkilä and P. M. Pihko, *J. Org. Chem.*, 2006, **71**, 2538–2541.
71 Y. Hu, Y.-H. He and Z. Guan, *Catal. Commun.*, 2010, **11**, 656–659.
72 R. C. M. Alves Sobrinho, P. M. de Oliveira, C. R. Montes D'Oca, D. Russowsky and M. G. Montes D'Oca, *RSC Adv.*, 2017, **7**, 3214–3221.
73 A. T. Nguyen Tran, Z. Wu, D. T. M. Chung, P. Nalaoh and J. S. Lindsey, *New J. Chem.*, 2023, **47**, 13626–13637.
74 J. A. Malona, J. M. Colbourne and A. J. Frontier, *Org. Lett.*, 2006, **8**, 5661–5664.
75 H. Mazaki, T. Watanabe, T. Takahashi, A. Struck and H. Scheer, *Bull. Chem. Soc. Jpn.*, 1992, **65**, 3080–3087.
76 Y. Saga and S. Nakagawa, *J. Porphyrins Phthalocyanines*, 2020, **24**, 499–504.
77 C. J. Gisriel, C. Azai and T. Cardona, *Photosynth. Res.*, 2021, **149**, 329–343.
78 G. S. Orf, C. Gisriel and K. E. Redding, *Photosynth. Res.*, 2018, **138**, 11–37.
79 M. R. Wasielewski and W. A. Svec, *J. Org. Chem.*, 1980, **45**, 1969–1974.
80 M. Itoh, D. Hagiwara and J. Notani, *Synthesis*, 1975, 456–458.
81 S. Takano, T. Sugihara and K. Ogasawara, *Synlett*, 1991, 279–282.
82 M. R. Wasielewski, *Tetrahedron Lett.*, 1977, **18**, 1373–1376.
83 J. H. C. Smith and A. Benitez, in *Modern Methods of Plant Analysis*, ed. K. Paech and M. V. Tracey, Springer Berlin Heidelberg, Berlin, Heidelberg, 1955, vol. 4, pp. 142–196.
84 H. Falk, G. Hoornaert, H. Isenring and A. Eschenmoser, *Helv. Chim. Acta*, 1975, **58**, 2347–2357.
85 H. Scheer and J. J. Katz, *J. Am. Chem. Soc.*, 1978, **100**, 561–571.
86 J. Dandler, B. Wilhelm and H. Scheer, *Photochem. Photobiol.*, 2010, **86**, 182–193.
87 N. Srinivasan, C. A. Haney, J. S. Lindsey, W. Zhang and B. T. Chait, *J. Porphyrins Phthalocyanines*, 1999, **3**, 283–291.
88 C. D. Calvano, G. Ventura, M. Trotta, G. Bianco, T. R. I. Cataldi and F. Palmisano, *J. Am. Soc. Mass Spectrom.*, 2017, **28**, 125–135.
89 E. Walter, J. Schreiber, E. Zass and A. Eschenmoser, *Helv. Chim. Acta*, 1979, **62**, 899–920.
90 M. Meyer, H. Scheer and J. Breton, *FEBS Lett.*, 1996, **393**, 131–134.
91 C. Houssier and K. Sauer, *J. Am. Chem. Soc.*, 1970, **92**, 779–791.
92 A. N. Kozyrev, Y. Chen, L. N. Goswami, W. A. Tabaczynski and R. K. Pandey, *J. Org. Chem.*, 2006, **71**, 1949–1960.
93 G. Zheng, WO 2006/073419, 2006.

94 Á. Roxin, J. Chen, A. S. Paton, T. P. Bender and G. Zheng, *J. Med. Chem.*, 2014, **57**, 223–237.
95 Á. Roxin, T. D. MacDonald and G. Zheng, *J. Porphyrins Phthalocyanines*, 2014, **18**, 188–199.
96 R. G. Brereton and J. K. M. Sanders, *J. Chem. Soc. Perkin Trans. I*, 1983, 423–430.
97 R. G. Brereton and J. K. M. Sanders, *J. Chem. Soc. Perkin Trans. I*, 1983, 435–437.
98 L. Limantara, P. Koehler, B. Wilhelm, R. J. Porra and H. Scheer, *Photochem. Photobiol.*, 2006, **82**, 770–780.
99 K. Hyvärinen and P. H. Hynninen, *Res. Adv. Org. Bioorg. Chem.*, 2001, **1**, 1–19.
100 (*a*) CCDC 2519170: Experimental Crystal Structure Determination, 2025, DOI: 10.5517/ccdc.csd.cc2qkdk8; (*b*) CCDC 2519171: Experimental Crystal Structure Determination, 2025, DOI: 10.5517/ccdc.csd.cc2qkdl9; (*c*) CCDC 2519172: Experimental Crystal Structure Determination, 2025, DOI: 10.5517/ccdc.csd.cc2qkdmb.